

Proposed Applications of Graphene for Millimeter-wave Passive Networks

Ahmed M. Attiya

Electronics Research Institute
El-Tahreer St., Dokki, Giza, Egypt, 12622
attiya@eri.sci.eg

Abstract - This paper presents a full wave analysis of a rectangular wave guide loaded with a double-layered graphene sheet mounted on a finite-thickness dielectric slab. The chemical potential of the graphene sheet is controlled by the applied electrical potential between the two layers of the graphene sheet which subsequently controls the surface conductivity of the graphene sheet. This property is found to have a significant effect at frequencies above 50 GHz. By controlling the conductivity of the graphene sheet it would be possible to control the amplitude and phase of the transmission and refraction coefficients along the waveguide section. This feature can be used in different applications in mm-wave range like switches, attenuators, filters, resonators and modulators.

Keywords: Graphene; Nanotechnology; Millimeter-wave.

1. Introduction

Graphene is a one-layer of carbon atoms arranged in a hexagonal 2D lattice. Early theoretical study of this configuration shows that this structure has unique physical properties including quite high electron mobility (Wallace, 1947). However, the main interest in graphene has been mainly increased in last two decades after discovering experimentally related nano structures like carbon nanotubes and quantum dots. However, the graphene sheet itself could be extracted for first time by Novoselov et al. (2004). More recently Li et al. (2009) introduced an efficient technique for synthesizing large-area graphene sheets of the order of centimeters on copper substrates. This discovery was the introduction for a huge research in different areas related to the possibility of using this one-layer carbon atoms in different applications.

One of the main properties of graphene sheet is that its surface conductivity can be tuned by applying normal electric and/or magnetic fields (Gusynin et al. 2007) (Hanson 2008a,2008b). This property makes graphene sheets are good candidate for tunable devices in mm-waves, THz and infrared frequency ranges.

In this paper we present an analytical solution for the problem of a rectangular waveguide loaded with a double-layered graphene diaphragm as shown in Fig. 1. The graphene diaphragm has a width $w_1 = a - w$ and is mounted on a dielectric slab of thickness d . This graphene diaphragm is composed of two graphene sheets separated by a thin layer Aluminum oxide of thickness t which is much smaller than the thickness of the supporting dielectric slab such that the double-layered graphene sheet is assumed to be of zero thickness in calculations. The thickness t is conventionally about 5-20 nm (Jablan et al. 2013, Svintsov et. al. 2013, Tamagnone et al. 2012, Filter et. al 2013, Gómez-Díaz et al. 2013, Liu et al. 2012). The conductivity of this double layered graphene sheet is approximated as twice the conductivity of a single graphene sheet (Tamagnone et al. 2012). The advantage of this double-layered configuration is that by applying a potential difference between the two layers of the graphene sheets, a normal electric field is introduced between them. Thus, by controlling the applied voltage between the two graphene sheets, it would be possible to tune the conductivity of the diaphragm which would enable controlling the scattering parameters of the waveguide section. In Sec. II, we present the basic theory of the problem. Section III shows results and discussions and finally Sec. IV presents the conclusion.

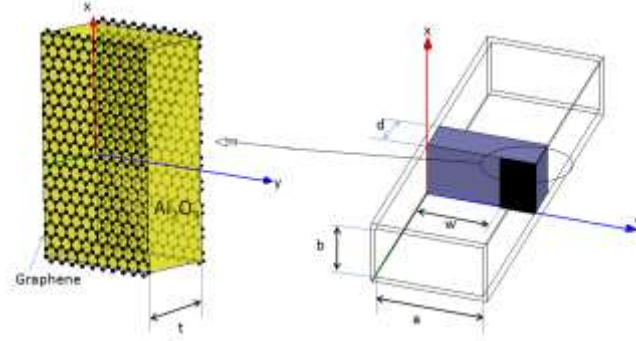


Fig. 1. Geometry of the problem.

2. Theory and Analysis

2. 1. Electrodynamic Conductivity of Graphene

The surface conductivity of a graphene sheet in the absence of a biasing magnetostatic field is given by (Hanson 2008b):

$$\sigma(\mu_c(E_0)) = \frac{je^2(\omega-2j\Gamma)}{\pi\hbar^2} \left[\frac{1}{(\omega-2j\Gamma)^2} \int_0^\infty \epsilon \left(\frac{\partial f_d(\epsilon)}{\partial \epsilon} - \frac{\partial f_d(-\epsilon)}{\partial \epsilon} \right) d\epsilon - \int_0^\infty \frac{f_d(-\epsilon) - f_d(\epsilon)}{(\omega-2j\Gamma)^2 - 4(\epsilon/\hbar)^2} d\epsilon \right], \quad (1)$$

where e is the electron charge, ω is the operating angular frequency, $\Gamma = 1/2\tau$ is the electron scattering rate, τ is the electron scattering time which is nearly 3ps in graphene sheet (Hanson, 2008b), μ_c is the chemical potential, E_0 is the applied biasing electrostatic field normal to the plane of the graphene sheet and f_d is the Fermi-Dirac distribution function given by:

$$f_d(\epsilon) = \left(e^{(\epsilon - \mu_c)/k_B T} + 2 \right)^{-1} \quad (2)$$

where k_B is Boltzmann's constant and T is the absolute temperature which equals 300 K at room temperature.

The chemical potential and subsequently the surface conductivity of the graphene sheet depend on the doping and the applied normal electric field. The relation between the chemical potential and the normal electric field is given by (Hanson 2008b):

$$E_0 = \frac{e}{\pi\epsilon_0\epsilon_r\epsilon_{eff}\hbar^2v_F^2} \int_0^\infty \epsilon (f_d(\epsilon) - f_d(\epsilon + 2\mu_c)) d\epsilon \quad (3)$$

where \hbar is the reduced Planck's constant, $v_F \cong 10^6 m/s$ is the electron's energy-independent velocity and $\epsilon_{r\,eff} \cong (\epsilon_r + 1)/2$ is the effective relative permittivity around the graphene sheets.

The dependence on the electric field introduces the possibility of using graphene sheets as tunable component by varying its surface conductivity. However, the required applied electric field to introduce a significant change in the surface conductivity is of order volts per nanometer (Hanson 2008a,2008b) which requires either high electric field or quite small distance between the corresponding plates which introduce this tuning electric field. For practical applications, two graphene sheets separated by a thin layer of Aluminum oxide of order 5-20 nm are used (Tamagnone et al. 2012). For this configuration the equivalent conductivity of the two-layer graphene sheet can be controlled by applying a voltage of amplitude less than 20 volts. This configuration is used as an optical modulator (Liu et al. 2012) and THz plasmonic antenna. In this case the equivalent conductivity of the double-layered graphene sheet is (Tamagnone et al. 2012):

$$\sigma_g = 2\sigma(\mu_c(E_0)) \quad (4)$$

2. 2. Analysis of a Rectangular Waveguide with a Diaphragm of Finite Conductivity

In this section we present modal solution of a rectangular waveguide with a diaphragm of finite conductivity mounted on a dielectric slab as shown in Fig. 1. Assuming that the incident field is the dominant TE₁₀ mode and the fields due to the discontinuity are presented in terms of higher TE modes only, one can represent the transverse electric fields in all regions as follows (Collin, 1960), (Lioubtchenko et al. 2003):

$$E_x(y, z) = \sin \frac{\pi y}{a} e^{-\gamma_1^0 z} + \sum_{n=1}^{\infty} A_n \sin \frac{n\pi y}{a} e^{\gamma_n^0 z}, \quad z \leq 0 \quad (5)$$

$$E_x(y, z) = \sum_{n=1}^{\infty} C_n \sin \frac{n\pi y}{a} e^{-\gamma_n^1 z} + D_n \sin \frac{n\pi y}{a} e^{\gamma_n^1 z}, \quad 0 \leq z \leq d \quad (6)$$

$$E_x(y, z) = \sum_{n=1}^{\infty} B_n \sin \frac{n\pi y}{a} e^{-\gamma_n^0 z}, \quad z \geq d \quad (7)$$

where $\gamma_n^i = \sqrt{\left(\frac{n\pi}{a}\right)^2 - k_i^2}$, $k_0 = \omega/c$, $k_1 = \sqrt{\epsilon_r} k_0$, ϵ_r is the relative dielectric constant of the supporting dielectric layer. In this case A_1 represents S_{11} and B_1 represents S_{21} . The transverse magnetic fields can be obtained in terms of the transverse electric fields as $H_y = (j/\omega\mu)\partial E_x/\partial z$. For computational purpose, the above infinite summations in (5)-(7) is truncated at N . The boundary conditions of the problem are

$$E_x(y, z = 0^-) - E_x(y, z = 0^+) = 0 \quad (8)$$

$$E_x(y, z = d^-) - E_x(y, z = d^+) = 0 \quad (9)$$

$$H_y(y, z = d^-) - H_y(y, z = d^+) = 0 \quad (10)$$

$$H_y(y, z = 0^+) - H_y(y, z = 0^-) = -\sigma(y)E_x(y, z = 0) \quad (11)$$

where $\sigma(y) = \sigma_g U(y - w)$, and σ_g is given by (4) where $U(\)$ is unit step function. By using the orthogonality of the modes and applying the boundary conditions in (8-11), one can formulate the problem as a set of linear equations as follows:

$$\begin{bmatrix} \mathbf{I} & \mathbf{0} & -\mathbf{I} & -\mathbf{I} \\ \mathbf{0} & -\mathbf{E}_0^- & \mathbf{E}_1^- & \mathbf{E}_1^+ \\ \mathbf{0} & \Lambda^0 \mathbf{E}_0^- & -\Lambda^1 \mathbf{E}_1^- & \Lambda^1 \mathbf{E}_1^+ \\ \Lambda^0 + j\omega\mu\sigma_g \mathbf{Y} & \mathbf{0} & \Lambda^1 & -\Lambda^1 \end{bmatrix} \begin{bmatrix} \mathbf{A} \\ \mathbf{B} \\ \mathbf{C} \\ \mathbf{D} \end{bmatrix} = \begin{bmatrix} \mathbf{p} \\ \mathbf{o} \\ \mathbf{o} \\ \mathbf{g} \end{bmatrix} \quad (12)$$

where $\Lambda^0, \Lambda^1, \mathbf{E}_1^-, \mathbf{E}_1^+$ and \mathbf{E}_0^- are diagonal matrices of $\gamma_m^0, \gamma_m^1, e^{-\gamma_m^1 d}, e^{\gamma_m^1 d}$ and $e^{-\gamma_m^0 d}$ respectively where $m = 1, 2, 3, \dots, N$. \mathbf{I} and $\mathbf{0}$ are unity and zero matrices respectively of order N . \mathbf{Y} is as square matrix of order N of elements $Y_{mn} = \frac{2}{a} \int_w^a \sin \frac{n\pi y}{a} \sin \frac{m\pi y}{a} dy$ where $m, n = 1, 2, 3, \dots, N$. \mathbf{p} is a vector of N elements where $p_m = -\delta(m - 1)$, and \mathbf{g} is a vector of N elements where $g_m = \gamma_1^0 \delta(m - 1) - j\omega\mu\sigma_g Y_{m1}$. Finally, \mathbf{o} is a vector of N zero elements. By solving (12) one can obtain the amplitudes of the field components in all regions inside the waveguide section and the corresponding S parameters.

3. Results and Discussions

At the beginning we studied the relation between the chemical potential μ_c and the applied normal electric field E_0 by using (3). By applying the linear relation between the applied electric field and the corresponding applied voltage, it would be possible to obtain direct relation between the applied voltage and the chemical potential. Figure (2) shows the relation between the applied voltage and the chemical

potential for the separation layer of thickness 5 nm between the two graphene sheets. It can be noted that by increasing the applied voltage the chemical potential is increased. This increase has a higher rate and higher non-linearity for chemical potential below 0.4 eV. For higher chemical potential, the rate of change with applied voltage becomes more linear.

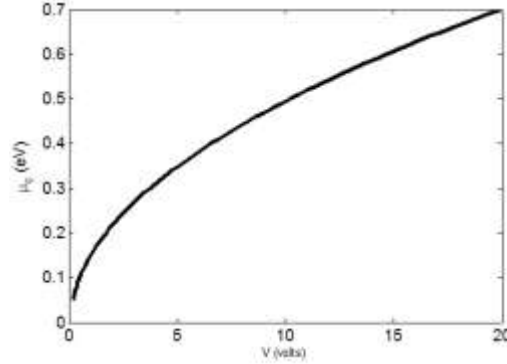


Fig. 2. Chemical potential of a graphene sheet as function of applied voltage where the applied voltage introduces normal electric field $E_0 = V/t$. The thickness t is 5 nm.

Figure 3 shows the conductivity of the double-layered graphene layer as function of the frequency. The chemical potential is controlled by applying a normal electric field as discussed in Fig. 2. The present results are shown as functions of the applied electric voltage for the proposed separation distance ($t = 5$ nm) between the two graphene sheets. It can be noted that conductivity is increased non-linearly by increasing the applied. It can also be noted that the magnitude of the imaginary part of the surface conductivity becomes greater than the real part above nearly 50 GHz.

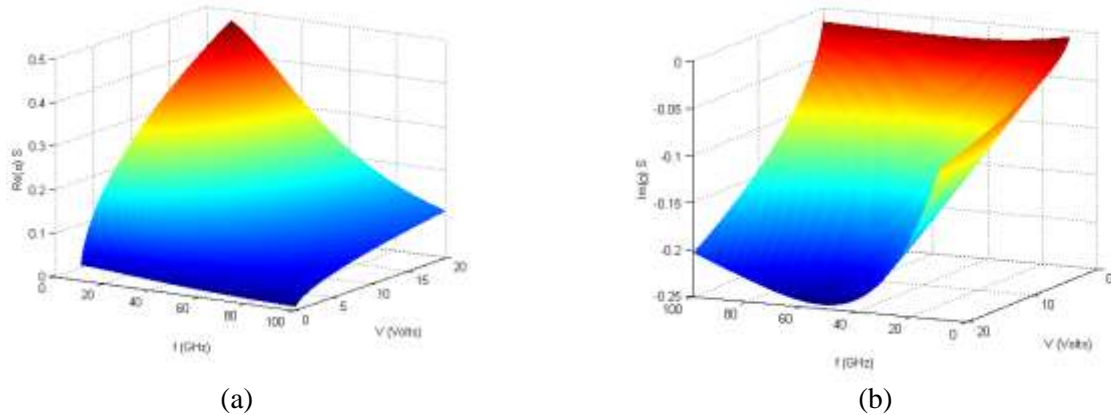


Fig. 3. (a) Real and (b) Imaginary parts of the conductivity of a double-layered graphene sheet as functions of the operating frequency and the applied normal electric field $E_0 = V/t$. The thickness t is 5 nm.

This double-layered graphene sheet is inserted as a diaphragm inside a rectangular waveguide as shown in Fig. 1. For the present case the waveguide is assumed to be WR-12 with inner dimensions $a = 3.0988$ mm and $b = 1.5494$ mm. The conventional operating frequency of this waveguide in unloaded case with its dominant TE₁₀ mode is from 60 to 90 GHz. The supporting dielectric slab is Teflon with $\epsilon_r = 2.1$ and $\tan \delta = 0.001$. The width of the double-layered graphene sheet is 1mm. Thus w in Fig. 1. is 2.0988 mm. Figure 4 shows the transmission and reflection coefficients for two values of chemical potentials 0.05 eV and 0.5 eV which correspond to applied DC voltages between the two layers of the graphene sheet 0.5V and 12 V respectively. The thickness of the dielectric substrate is $d = 1$ mm in Fig. 4-a and $d = 1.5$ mm in Fig. 4-b. It can be noted that the presence of the graphene sheet introduce

resonance effect in the S parameters. The chemical potential of the graphene sheet has effects on both amplitude and resonance frequency as shown in Fig. 4. It can also be noted that the resonance frequency is decreased by increasing the thickness of the dielectric slab. The slight change of the resonant frequency as a function of changing the chemical potential of the graphene sheet can introduce a significant difference in the transmission coefficient. For example, in Fig. 4-a, the transmission coefficient at applied DC voltage 0.5 V at 88.15 GHz is nearly -5dB, while at applied DC voltage 12 V at the same frequency is about -20.5dB. This means that this configuration can be used as a switch at this frequency with an On/Off ratio about 15dB. Similar property can also be noted in Fig. 4-b at 80.65 GHz. This property can also be useful in amplitude shift keying modulation. It can also be noted that, slightly near the resonance frequency, the amplitude of the transmission coefficient changes as a function of the chemical potential of the graphene sheet. This property can be useful to introduce variable attenuator or amplitude modulation.

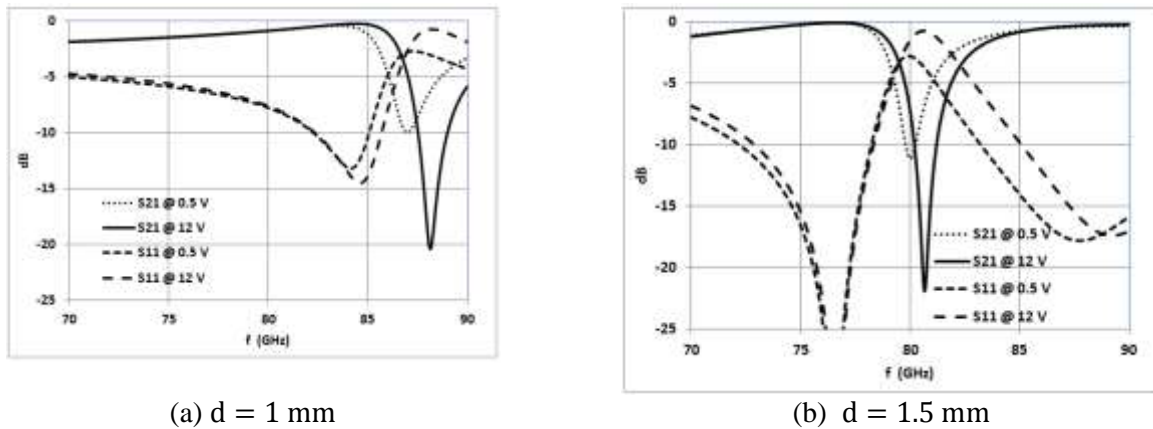


Fig. 4. Amplitudes of reflection and transmission coefficients for different values of applied voltage between the two graphene sheets.

Finally, Fig. 5 shows the phase of the transmission coefficients for the problem of Fig. 4-b. It can be noted that away of the resonance frequency in the range from 85 to 90 GHz, the amplitude of the transmission coefficient is nearly independent on the chemical potential of the graphene sheet as shown in Fig. 4-b. However, for the same frequency range, the change of the chemical potential of the graphene sheet has an effect on the phase of the transmission coefficient as shown in Fig. 5. This property can be useful to introduce phase shifter or phase modulator.

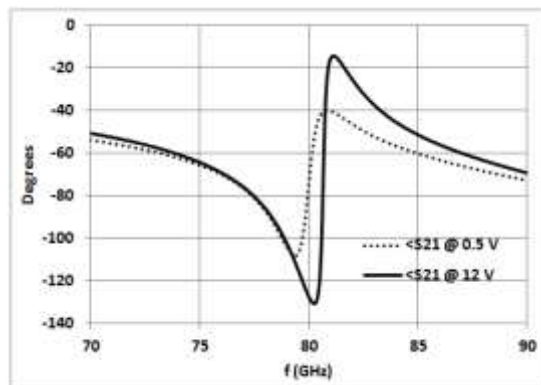


Fig. 5. Amplitudes of reflection and transmission coefficients for different values of applied voltage between the two graphene sheets. $d = 1.5 \text{ mm}$

4. Conclusion

In this paper we present full wave analysis of a rectangular waveguide loaded with a double-layered

graphene diaphragm mounted on a dielectric slab. The graphene sheet is modeled as a finite conducting. The conductivity of the graphene sheet depends on its chemical potential which is a function of the normal applied electric field between the two graphene layers. The graphene diaphragm controls the transmission and reflection coefficients of the waveguide section. By controlling the conductivity of the graphene sheet, it is found that it would be possible to control the amplitude and phase of reflection and transmission coefficients. With appropriate control it would be possible to use this property for different applications like switches, variable attenuators, resonators, phase shifters and modulators in millimeter-wave range, specifically above 50 GHz.

References

- Collin R. E. (1960). "Field Theory of Guided Waves" McGraw-Hill Book Co., New York, 1960.
- Filter R., Farhat M., Steglich M., Alaei R., Rockstuhl C., Lederer F. (2013). Tunable graphene antennas for selective enhancement of THz-emission. *Optics Express*, 21, 3737-3745.
- Gómez-Díaz J.S., Perruisseau-Carrier J. (2013). Graphene-based plasmonic switches at near infrared frequencies. *Opt. Express*, 21, 15490-15504.
- Gusynin V.P., Sharapov S.G., Carbotte J.P. (2007). Magneto-optical conductivity in graphene. *Journal of Physics: Condensed Matter*, 19, 026222.
- Hanson G. (2008a). Dyadic green's functions and guided surface waves for a surface conductivity model of graphene. *J. Appl. Phys.*, 103, 064 302-064 302.
- Hanson G.W. (2008b). Dyadic Greens functions for an anisotropic, non-local model of biased graphene. *IEEE Trans. Antennas Propag.*, 56, 747-757.
- Jablan M., Buljan H., Soljačić M. (2009). Plasmonics in graphene at infrared frequencies. *Physical Review B* vol. 80, 245435
- Li X., Cai W., An J., Kim S., Nah J., Yang D., Piner R., Velamakanni A., Jung I., Tutuc E., Banerjee S.K., Colombo L., Ruoff R.S. (2009). Large-Area Synthesis of High-Quality and Uniform Graphene Films on Copper Foils, *Science*, 324, 1312m.
- Lioubtchenko D., Tretyakov S., Dudorov S. (2003) "Millimeter-Wave Waveguides" Kluwer Academic Publishers 2003.
- Liu M., Yin X., Zhang X. (2012). Double-Layer Graphene Optical Modulator. *Nano Lett.*, 12, 1482–1485.
- Novoselov K. S., Geim A.K., Morozov S. V., Jiang, D., Zhang, Y., Dubonos S.V., Grigorieva I.V., and Firsov A.A. (2004). Electric field effect in atomically thin carbon films. *Science*, 306, 666–669.
- Svintsov D., Vyurkov V., Ryzhii V., Otsuji T. (2013). Voltage-controlled surface plasmon-polaritons in double graphene layer structures. *J. Appl. Phys.* 113, 053701.
- Tamagnone M., Gómez-Díaz J.S., Mosig J.R., Perruisseau-Carrier J. (2012). Reconfigurable terahertz plasmonic antenna concept using a graphene stack. *Appl. Phys. Lett.*, vol. 101, 214102.
- Wallace P.R (1947). The band theory of graphite. *Phys. Rev.*, 71, 622–634.